

# Training-free Adjustable Polynomial Graph Filtering for Ultra-fast Multimodal Recommendation

Yu-Seung Roh<sup>a</sup>, Joo-Young Kim<sup>b</sup>, Jin-Duk Park<sup>c</sup> and Won-Yong Shin<sup>a,\*</sup>

<sup>a</sup>*School of Mathematics and Computing (Computational Science and Engineering), Yonsei University, Seoul, 03722, Republic of Korea*

<sup>b</sup>*Graduate School of Data Science, Seoul National University, Seoul, 08826, Republic of Korea*

<sup>c</sup>*NAVER Corporations, Bundang, 13561, Republic of Korea*

## ARTICLE INFO

*Keywords:*

Graph filtering

Modality

Multimodal recommendation

Polynomial graph filter

Recommender system

## ABSTRACT

Multimodal recommender systems improve the performance of canonical recommender systems with no item features by utilizing diverse content types such as text, images, and videos, while alleviating inherent sparsity of user–item interactions and accelerating user engagement. However, current neural network-based models often incur significant computational overhead due to the complex training process required to learn and integrate information from multiple modalities. To address this challenge, we propose **MultiModal-Graph Filtering (MM-GF)**, a *training-free* method grounded in *graph filtering (GF)* for efficient and accurate multimodal recommendations. Specifically, MM-GF first constructs multiple similarity graphs for two distinct modalities as well as user–item interaction data. Then, MM-GF optimally fuses these multimodal signals using a polynomial graph filter that allows for precise control of the frequency response by adjusting frequency bounds. Furthermore, the filter coefficients are treated as hyperparameters, enabling flexible and data-driven adaptation. Extensive experiments on real-world benchmark datasets demonstrate that MM-GF not only improves recommendation accuracy by up to 22.25% compared to the best competitor but also dramatically reduces computational costs by achieving **the runtime of less than 10 seconds**.

## 1. Introduction

### 1.1. Background and Motivation

Recently, multimodal recommender systems (MRSs) have garnered significant attention due to their ability to accommodate diverse item information from multiple modalities for enhanced recommendation performance. Compared to canonical recommender systems (He et al., 2020; Ranjbar et al., 2015; Valcarce et al., 2019) with no item features (referred to as single-modal recommender systems), MRSs can capture and leverage precise item information (e.g., textual and/or visual features) for recommendations, thereby enhancing the overall capabilities of recommender systems (He and McAuley, 2016b; Wei et al., 2020). Notably, while single-modal recommender systems often struggle with sparsity of user–item interactions, MRSs can overcome this limitation by utilizing multimodal features of items. Due to these advantages, MRSs (Yu et al., 2023; Zhang et al., 2021; Zhou and Shen, 2023; Zhou et al., 2023b) are shown to substantially outperform single-modal recommendation methods based on collaborative filtering that rely solely on historical user–item interactions.

Various MRSs have been developed to improve recommendation performance. In particular, thanks to the expressive capability via message passing in graph convolutional networks (GCNs) (Kipf and Welling, 2017), attention has been paid to GCN-based MRSs (Wei et al., 2020; Yu et al., 2023; Zhang et al., 2021; Zhou and Shen, 2023; Zhou et al., 2023b). For example, prior studies on MRSs learned GCNs separately to process different modalities, distinct from user–item interactions (Kim et al., 2024; Wei et al., 2020; Zhang et al., 2021), or constructed an item–item similarity graph based on multimodal information (i.e., multimodal features of items) and then applied GCNs to process the similarity graph (Zhang et al., 2021).

On one hand, user preferences tend to shift quickly under the influence of trends, personal situations, and exposure to new content (Ju et al., 2015; Pereira et al., 2018); hence, recommender systems need to be flexible to adapt to such dynamic preferences. Especially in environments where the training and inference speed is crucial, model runtime

\*Corresponding author

✉ wy.shin@yonsei.ac.kr (W. Shin)

ORCID(s): 0000-0002-6533-3469 (W. Shin)

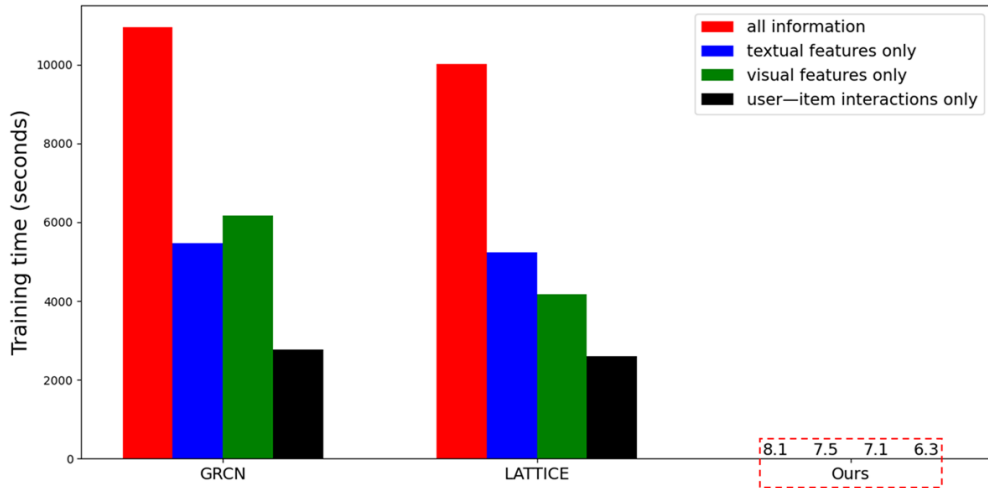


**Figure 1:** Training time comparison of various MRSs under different degrees of modality information on the Baby dataset. Here, the end-to-end processing time is measured for our method that does not need any training process.

can become a significant bottleneck. In this context, incorporating additional information (i.e., multimodal features of items) into modeling significantly increases computational overhead for GCN-based MRSs. Consequently, MRSs learn multimodal information through GCNs, naturally leading to escalation of training time for GCNs with the increased number of modalities. Figure 1 illustrates how the training time (in seconds) of various MRSs behaves according to different degrees of modality information on the Baby dataset (one of well-known benchmark datasets for MRSs). As shown in the figure, the training time of GRCN (Wei et al., 2020) and LATTICE (Zhang et al., 2021) for processing all multimodal information is considerably high, which signifies the significant computational cost of GCN-based models when such data are integrated. Thus, although using GCN-based MRSs (e.g., (Wei et al., 2020; Zhang et al., 2021)) is promising, we face practical challenges in computational complexity especially for the case when the speed at which recommender systems update their models is of paramount importance due to the dynamics of user preferences.

On the other hand, recent studies on single-modal recommender systems (Liu et al., 2023; Park et al., 2024; Shen et al., 2021; Xia et al., 2022) have adopted the *training-free* graph filtering (GF) (also known as graph signal processing) mechanism due to its simplicity and effectiveness. Such GF is a fundamental operation enabling the manipulation of signals defined over the nodes based on the underlying graph topology (Defferrard et al., 2016; Isufi et al., 2024). A pioneering study on training-free GF is GF-CF (Shen et al., 2021), which presented a novel approach to constructing an item-item similarity graph and applying GF that does not necessitate model training to enhance recommendation performance. Subsequent studies (Liu et al., 2023; Xia et al., 2022) have been introduced to further enhance the effectiveness of GF-based recommender systems. Additionally, recent studies (Kim et al., 2025; Park et al., 2024, 2025) proposed a powerful normalization scheme that enables adjustable influence between users and items, while introducing tunable hyperparameters to mitigate over-smoothing and under-smoothing and employing polynomial graph filters that avoid explicit eigendecomposition.

Despite these advances, the GF-based recommendation methods in (Kim et al., 2025; Park et al., 2024, 2025) present a key limitation from the perspective of frequency analysis. Normalization techniques in (Liu et al., 2023; Shen et al., 2021; Xia et al., 2022) ensure that all eigenvalues of the underlying item-item similarity graph lie within the interval  $[0, 1]$ , providing a stable theoretical foundation for designing polynomial filters in the frequency domain. In contrast, the normalization and additional adjustment process in (Kim et al., 2025; Park et al., 2024, 2025) does not enforce this spectral constraint, allowing eigenvalues to extend beyond the unit interval, which distorts the intended frequency response. This effect is magnified on multimodal information due to heterogeneous characteristics, resulting in greater spectral instability than the case of user-item interactions. Additionally, such an effect can be amplified with higher-order polynomials, disproportionately emphasizing components tied to large-magnitude eigenvalues and further degrading frequency control. The aggregation of multiple out-of-band components generates spurious, highly distorted signals. These limitations underscore the need for a rigorous and sophisticated polynomial graph filtering strategy tailored for recommendation systems. Moreover, their polynomial filters in (Kim et al., 2025; Park et al.,

**Table 1**  
Summary of notations.

Notation	Description
$\mathcal{G}$	Underlying graph
$\mathcal{V}$	Set of nodes in $\mathcal{G}$
$\mathcal{E}$	Set of edges in $\mathcal{G}$
$\mathcal{U}$	Set of users
$\mathcal{I}$	Set of items
$R$	user–item rating matrix (interactions)
$\mathcal{M}$	Set of multimodal information (i.e., textual and visual information)
$L$	Graph Laplacian of $\mathcal{G}$
$U$	Set of eigenvectors of $L$
$\Lambda$	Set of eigenvalues of $L$
$\lambda_{min}$	Minimum eigenvalue of $\Lambda$
$\lambda_{max}$	Maximum eigenvalue of $\Lambda$
$x$	Graph signal
$D$	Diagonal degree matrix
$P$	Item–item similarity matrix

2024, 2025) were analytically derived from a *fixed* frequency response function, which lacks flexibility. This limitation underscores the need for a more adjustable and theoretically grounded filtering strategy for recommender systems.

## 1.2. Main Contributions

To tackle the aforementioned challenges, we propose MultiModal-Graph Filtering (MM-GF), a new GF method tailored for MRSs. Specifically, MM-GF constructs multiple similarity graphs derived from user–item interaction data and two distinct modalities. Unlike user–item interactions, multimodal information (i.e., multimodal features of items) often contains *outliers* and *negative values*, which can make the resulting similarity graphs highly sensitive to noise or prone to singularities (e.g., division by zero during normalization). To mitigate these issues, MM-GF leverages similarity calculations within each modality, thereby capturing modality-specific item–item relationships in a stable manner.

In the GF process, we theoretically identify a critical issue in regard to eigenvalue bounds (see Section 4.1 for technical details). MM-GF employs a polynomial graph filter that enables *precise frequency control* by adjusting the spectral bounds, thereby eliminating the limitations associated with unbounded eigenvalues. The filter coefficients are treated as tunable hyperparameters, allowing for flexible, data-driven adaptation of the frequency response to match the spectral properties of a given dataset. This design facilitates seamless adaptation to diverse spectral properties of the given data, enhancing the filter’s effectiveness across diverse recommendation scenarios, and ultimately allowing MM-GF to optimally aggregate multimodal information.

Extensive experiments on various real-world datasets demonstrate that MM-GF achieves up to 22.25% higher accuracy and up to  $\times 100.4$  faster runtime compared to the best MRS competitor. In other words, MM-GF is not only extremely fast but also highly accurate, compared to the GCN-based MRSs harnessing computationally expensive model training.

Our contributions are summarized as follows:

- **Theoretical finding:** We theoretically investigate the impact of asymmetric normalization and adjustment on the eigenvalue bounds. This analysis reveals that even minor changes in normalization can significantly shift the spectral range, which in turn affects the stability of GF.
- **Methodology:** We devise MM-GF, a new and theoretically sound polynomial graph filter that precisely adjusts spectral bounds, ensuring accurate frequency design control and resolving the eigenvalue constraint issue in asymmetric graph constructions with adjustment parameters.
- **Extensive evaluation:** We carry out comprehensive experiments, which include cold-start and noisy feature settings, on three widely used benchmark datasets for MRSs. The results consistently demonstrate the effectiveness of MM-GF in terms of computational complexity and model accuracy, compared to GCN-based MRSs.

### 1.3. Organization and Notations

The remainder of this paper is organized as follows. In Section 2, we summarize prior work relevant to our study. Section 3 provides some preliminaries such as the notion of GF and the problem definition. Section 4 describes the technical details of the proposed MM-GF method. Extensive experimental results and analyses are presented in Section 5. Finally, we provide a summary and concluding remarks in Section 6.

Table 1 summarizes the notation that is used in this paper. This notation will be formally defined in the following sections when we introduce our methodology and technical details.

## 2. Related work

In this section, we review broad research lines related to our study, including 1) GF-based recommendation methods and 2) multimodal recommendation methods.

**GF-based recommendation.** In the context of GF, GCN (Kipf and Welling, 2017) is viewed as a parameterized convolutional filter for graphs. A notable GCN-based recommendation method is NGCF (Wang et al., 2019), which was proposed to learn suitable low-pass filters (LPFs) while capturing high-order collaborative signals present in user–item interactions. LightGCN (He et al., 2020) demonstrated strong performance by simplifying NGCF, removing both linear transformations and non-linear activations from its GCN layers. By bridging the gap between LightGCN and GF approaches, GF-CF (Xu et al., 2019) was introduced, offering satisfactory recommendation accuracy with minimal computational costs due to its training-free design and a closed-form solution for the infinite-dimensional LightGCN. As a follow-up study, PGSP (Liu et al., 2023) employed a mixed-frequency filter that integrates a linear LPF with an ideal LPF. Furthermore, in Turbo-CF (Park et al., 2024), polynomial LPFs were designed to retain low-frequency signals without an ideal LPF that requires costly matrix decompositions.

**Multimodal recommendation.** Studies on MRSs have been actively conducted to boost the performance of recommender systems by leveraging information of multimodal features of items (i.e., textual and visual features). Initially, VBPR (He and McAuley, 2016b) extended Bayesian personalized ranking (BPR) loss (Rendle et al., 2012) by utilizing visual features of items. Similarly as in other graph-based training models, GCNs have also gained attention due to their ability to seamlessly integrate multimodal information. For example, GRCN (Wei et al., 2020) was presented alongside GCNs that construct a refined user–item bipartite graph so as to identify false-positive interactions by utilizing multimodal information. LATTICE (Zhang et al., 2021) applied graph convolution operations to capture high-order item–item relationships and integrate them. BM3 (Zhou et al., 2023b) presented a self-supervised learning framework, bootstrapping latent representations of both user–item interactions and multimodal features, thus providing a simple yet efficient approach to recommendation. FREEDOM (Zhou and Shen, 2023) extended LATTICE (Zhang et al., 2021) by simplifying the construction of item–item similarity graphs and incorporating a degree-sensitive edge pruning method. In MGCN (Yu et al., 2023), noisy features was purified, the purified modality features of items and behavior features were enriched in separate views, and a behavior-aware fuser was designed to predict user preferences. LGMRec (Guo et al., 2024) exploited multimodal information through the construction of a hypergraph, which enables the joint modeling of various user preferences. PGL (Yu et al., 2025) enhanced user preference modeling by extracting principal subgraphs from user–item interactions and performing message passing to jointly capture global and local information for principal subgraphs.

## 3. Preliminaries

We provide some preliminaries such as the GF mechanism and the problem definition.

### 3.1. Notion of GF

We provide fundamental principles of GF (or equivalently, graph signal processing) (Ortega et al., 2018; Park et al., 2024; Shen et al., 2021). First, we consider an undirected graph  $\mathcal{G} = (\mathcal{V}, \mathcal{E})$ , which is represented by an adjacency matrix  $A$  that indicates the presence or absence of edges between nodes. The Laplacian matrix  $L$  of  $\mathcal{G}$  is defined as  $L = D - A$ , where  $D$  is the degree matrix of  $A$  (Grone and Merris, 1994). Meanwhile, a graph signal on  $\mathcal{G}$  is expressed as  $\mathbf{x} \in \mathbb{R}^{|\mathcal{V}|}$ , where each  $x_i$  indicates the signal strength at the corresponding node  $i$  in  $\mathbf{x}$ . The smoothness of a graph signal  $\mathbf{x}$  can be mathematically measured by

$$S(\mathbf{x}) = \sum_{i,j} A_{ij}(x_i - x_j)^2 = \mathbf{x}^T L \mathbf{x}, \quad (1)$$

where a smaller  $\frac{S(\mathbf{x})}{\|\mathbf{x}\|_2}$  indicates a smoother  $\mathbf{x}$ .

The graph Fourier transform (GFT) converts a graph signal into the frequency domain using the eigenvectors of the graph Laplacian  $L = U\Lambda U^T$ , where  $U \in \mathbb{R}^{|\mathcal{V}| \times |\mathcal{V}|}$  is the matrix whose columns correspond to a set of eigenvectors of  $L$  and  $\Lambda$  is a diagonal matrix containing the set of eigenvalues of  $L$ . Thus, the graph signal  $\mathbf{x}$  can be transformed into  $\hat{\mathbf{x}} = U^T \mathbf{x}$ , which utilizes the spectral characteristics of the underlying graph to examine the latent structure of the graph signal. The GFT is used to perform *graph convolution*, with the aid of *graph filters*, which is mathematically defined as follows.

**Definition 1** (Graph filter). The graph filter  $H(L)$  is defined as

$$H(L) = U \text{diag}(h(\lambda_1), \dots, h(\lambda_{|\mathcal{V}|})) U^T, \quad (2)$$

where  $h()$  is the frequency response function that maps eigenvalues  $\{\lambda_1, \dots, \lambda_{|\mathcal{V}|}\}$  of  $L$  to  $\{h(\lambda_1), \dots, h(\lambda_{|\mathcal{V}|})\}$ .

**Definition 2** (Graph convolution). The graph convolution of a signal  $\mathbf{x}$  and a graph filter  $H(L)$  is defined as

$$H(L)\mathbf{x} = U \text{diag}(h(\lambda_1), \dots, h(\lambda_{|\mathcal{V}|})) U^T \mathbf{x}. \quad (3)$$

### 3.2. Problem Definition

We formally present the problem of top- $K$  multimodal recommendations. First, let  $\mathcal{U}$  and  $\mathcal{I}$  denote the set of users and the set of items, respectively. A user–item rating matrix is denoted as  $R \in \mathbb{R}^{|\mathcal{U}| \times |\mathcal{I}|}$ , and  $\mathcal{M}$  is the set of multiple modalities. In this paper, we use the textual and visual features denoted as  $\mathcal{M} = \{\text{txt}, \text{img}\}$ . We denote the feature matrix of modality  $m \in \mathcal{M}$  as  $X^m \in \mathbb{R}^{|\mathcal{I}| \times d_m}$  for the dimensionality  $d_m$ . The objective of the multimodal recommendation task is to recommend top- $K$  items to each user using multimodal features of items as well as user–item interactions representing the ratings.

## 4. Methodology

In this section, we elaborate on the proposed MM-GF method as well as our research motivation.

### 4.1. Motivation and Challenges

Conventional training-free GF-based recommendation methods (Liu et al., 2023; Shen et al., 2021) start by constructing a graph structure, where nodes represent items and edges correspond to item–item similarities. The graph construction process is formulated as follows:

$$\tilde{P} = \tilde{R}^T \tilde{R}; \tilde{R} = D_r^{-1/2} R D_c^{-1/2}, \quad (4)$$

where  $\tilde{R}$  is the normalized rating matrix;  $D_r = \text{diag}(R\mathbf{1})$  and  $D_c = \text{diag}(\mathbf{1}^T R)$  are the diagonal degree matrices of users and items, respectively, for the all-ones vector  $\mathbf{1}$ ; and  $\tilde{P}$  is the adjacency matrix of the item–item similarity graph.

Recently, (Kim et al., 2025; Park et al., 2024, 2025) utilized asymmetric normalization on  $R$  to regularize the popularity of users or items before calculating  $\tilde{P}$ , which is formulated as follows:

$$\tilde{P} = \tilde{R}^T \tilde{R}; \tilde{R} = D_r^{-\alpha} R D_c^{\alpha-1}, \quad (5)$$

where  $\alpha \in [0, 1]$  is the hyperparameter to control the normalization among users and items. Intuitively, as  $\alpha$  decreases, the influence of popular items on  $\tilde{R}$  becomes weak. Additionally, to address over-smoothing or under-smoothing problems, an adjustment hyperparameter was adopted for the graph  $\tilde{P}$  as:

$$\tilde{P} = \tilde{P}^{os}, \quad (6)$$

where  $s$  is an adjustment parameter tunable on the validation set.

However, as critical issues, introducing two hyperparameters (i.e.,  $\alpha$  and  $s$ ) may alter the spectral characteristics of the underlying graph. Specifically, the work in (Shen et al., 2021) proved that all the eigenvalues of  $\tilde{P} = \tilde{R}^T \tilde{R}$  where  $\tilde{R} = D_r^{-0.5} R D_c^{-0.5}$  are in  $[0, 1]$ . Nonetheless, as long as parameters  $\alpha$  and  $s$  are concerned, one cannot always assure that  $\tilde{P}$  in Eqs. (5) and (6) satisfies the aforementioned condition in Section 1.1 (i.e., the unit interval of eigenvalues) when  $\alpha \neq 0.5$  and/or  $s \neq 1$ . In Figure 2, we present two cases: Case 1)  $\alpha = 0.5$  and  $s = 1$ , corresponding to symmetric

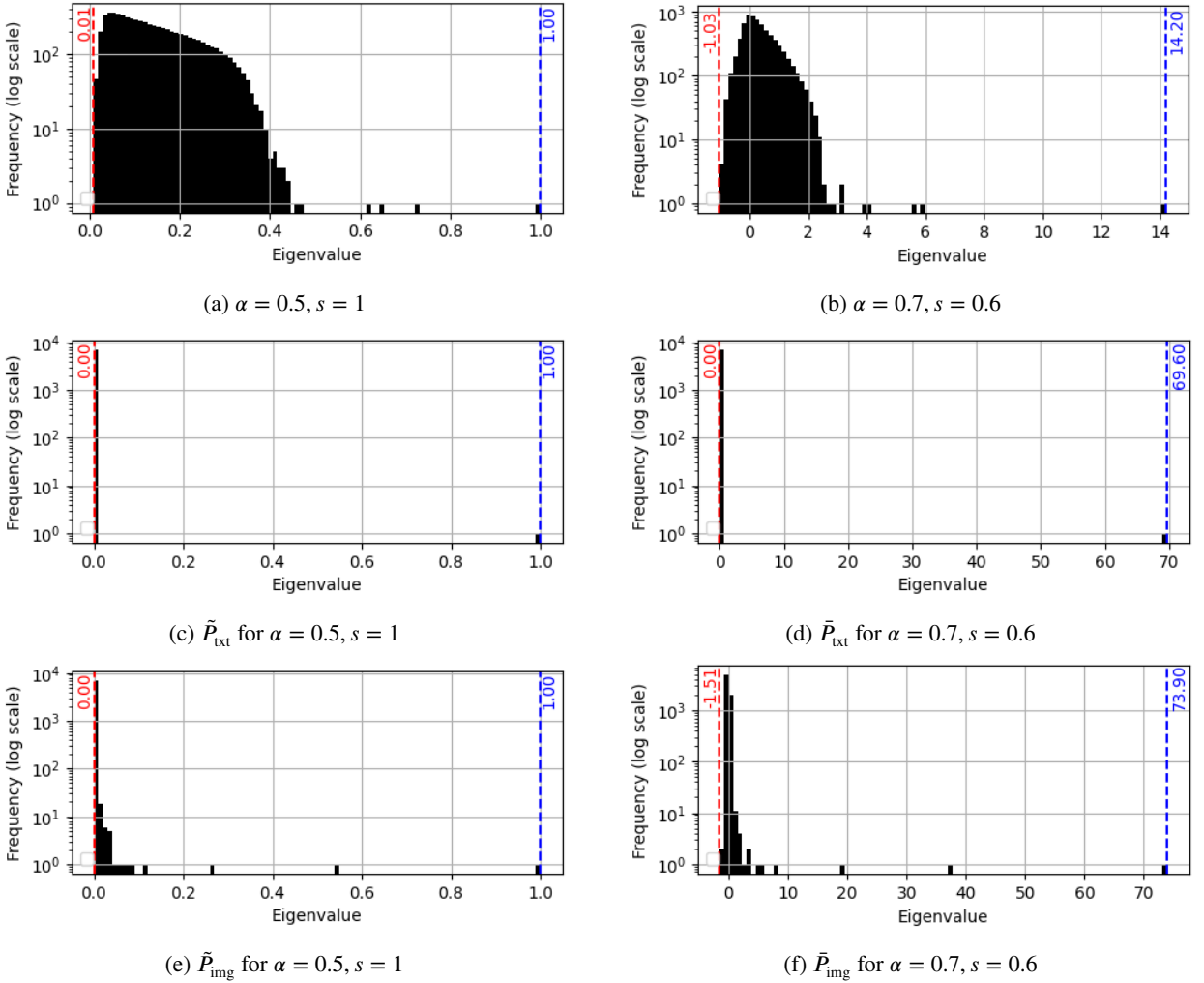


**Figure 2:** Histogram of eigenvalues for item–item similarity graphs constructed from user–item interactions and multimodal information on the Baby dataset. The left panels show the case of  $\alpha = 0.5$  and  $s = 1$ , corresponding to symmetric normalization, while the right panels show the case of  $\alpha = 0.7$  and  $s = 0.6$ , representing asymmetric normalization with an additional adjustment process. Red dashed lines indicate the minimum eigenvalue of each graph, while blue dashed lines indicate the maximum eigenvalue.

normalization, and Case 2)  $\alpha = 0.7$  and  $s = 0.6$ , corresponding to asymmetric normalization with an additional adjustment process. The observations from this figure pose practical challenges below.

- **User–item interactions.** In Figures 2a and 2b, each histogram illustrates the distribution of eigenvalues of two distinct item–item similarity graphs constructed by Case 1 and 2, respectively, for user–item interaction data on the Baby dataset. We observe from Figure 2a that all eigenvalues lie within the interval  $[0, 1]$  for  $\alpha = 0.5$  and  $s = 1$  whereas, for another setting (i.e.,  $\alpha = 0.7$  and  $s = 0.6$ ) in Figure 2b, they range approximately from  $-1$  to  $14$ , which violates the unit-interval condition of the eigenvalues.
- **Multimodal information.** Figures 2c–2f present histograms of eigenvalue distributions for the Baby dataset. Figures 2c and 2e illustrate Case 1, and Figures 2d and 2f illustrate Case 2, each representing the eigenvalue distribution of the corresponding item–item similarity graph in the multimodal graph structure. The maximum eigenvalues of  $\tilde{P}_{\text{txt}}$  and  $\tilde{P}_{\text{img}}$  are approximately  $70$ , as illustrated in Figures 2d and 2f, which is considerably larger than the case of user–item interactions. The use of such unbounded frequency components not only hinders the effectiveness of polynomial graph filters but also introduces a non-ideal outcome when integrating multiple graph filters.

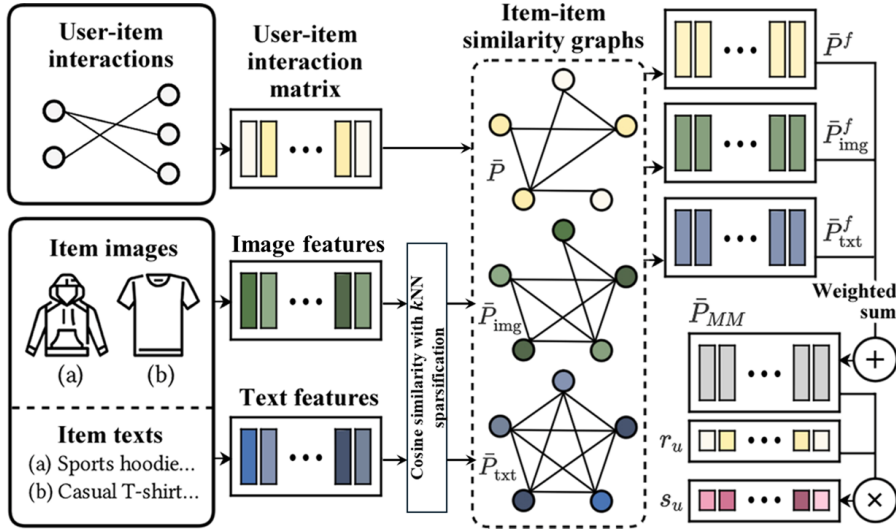


Figure 3: The schematic overview of MM-GF.

As observed in Figure 2, in general, if we naïvely adopt the polynomial LPFs used in (Kim et al., 2025; Park et al., 2024, 2025), then several issues arise. First, the filtered eigenvalues fall outside the range of  $[0, 1]$ . Symmetric normalization in (Liu et al., 2023; Shen et al., 2021; Xia et al., 2022) typically follow that the spectrum lies within this interval, which was proved by (Shen et al., 2021). When eigenvalues are mapped out of this range, the polynomial filter may yield inaccurate frequency responses, deviating from its designed frequency characteristics. Moreover, as the polynomial order increases, the filter response for large-magnitude eigenvalues can grow dramatically; this results in a disproportionate emphasis on certain frequency components, thereby degrading the model performance. For example, consider a polynomial LPF  $h(\lambda) = 1 - \lambda^2$ . In a bounded frequency range of  $[0, 1]$ , filtered values close to 0 correspond to high-frequency components, whereas those close to 1 correspond to low-frequency components. However, if the spectrum contains eigenvalues such as  $\lambda_1 \simeq -1$  and  $\lambda_2 \simeq 14$ , as shown in Figure 2b, then their corresponding filter responses become  $h(\lambda_1) \simeq 0$  and  $h(\lambda_2) \simeq -195$ , respectively. This phenomenon results in signals being assigned to anomalous frequencies instead of the targeted ones. Furthermore, this problem becomes particularly critical for multimodal information, where signals are more susceptible to distortion compared to the case of user—item interactions. For example, if the spectrum contains an eigenvalue  $\lambda_3 \simeq 70$ , as illustrated in Figures 2d and 2f, then its corresponding filter response becomes  $h(\lambda_3) \simeq -4899$ , leading to far more severe distortion than the case of user—item interactions. Ultimately, since MRSs require integrating signals across multiple modalities, aggregating such severely distorted signals can undermine the overall reliability of the recommendation process.

Addressing a different issue, while recent GF models (Kim et al., 2025; Park et al., 2024, 2025) demonstrated that a polynomial graph filter can be implemented as the form of  $\sum_{k=1}^K a_k \bar{P}^k$ , their empirical application was confined only to specific filters. This limited scope highlights a gap in the broader applicability of the GF methodology. Moreover, it is of paramount importance to effectively aggregate information across multiple modalities for accurate multimodal recommendations. In light of these challenges, a key question arises: "How can we design an efficient and effective GF method for multimodal recommendations by not only addressing the issue of filter design but also maximally exploiting heterogeneous characteristics across modalities?" To answer this question, we will outline the proposed MM-GF method tailored for multimodal recommendations in the following subsection.

## 4.2. Proposed Method: MM-GF

In this subsection, we describe the graph construction process and the filter design process in MM-GF. The schematic overview of MM-GF is illustrated in Figure 3. We provide the pseudocode of MM-GF in Algorithm 1, which summarizes the whole process.

**Algorithm 1** MM-GF

**Input:** User–item rating matrix  $R$ , textual feature matrix  $X^{\text{txt}}$ , visual feature matrix  $X^{\text{img}}$

**Hyperparameter:** Asymmetric normalization along users/items:  $\alpha$ , filter adjustment:  $s$ , balancing factors among the three item–item similarity graphs:  $\beta, \gamma$

- 1:  $\tilde{R} \leftarrow D_r^{-\alpha} R D_c^{\alpha-1}$  where  $D_r = \text{diag}(R\mathbf{1})$  and  $D_c = \text{diag}(\mathbf{1}^T R)$
- 2:  $\tilde{P} \leftarrow \tilde{R}^T \tilde{R}$
- 3:  $\tilde{P} \leftarrow \tilde{P}^{\circ s}$
- 4: **for**  $m \in \{\text{txt}, \text{img}\}$  **do**
- 5:    $S^m \leftarrow CS(X^m)$  where  $CS$  is cosine similarity
- 6:    $\hat{S}^m \leftarrow \text{top-}k(S^m)$  where  $\text{top-}k$  is  $\text{top-}k$  preservation
- 7:    $\tilde{S}_m \leftarrow D_{m,r}^{-\alpha} \hat{S}^m D_{m,c}^{\alpha-1}$  where  $D_{m,r} = \text{diag}(\hat{S}^m \mathbf{1})$  and  $D_{m,c} = \text{diag}(\mathbf{1}^T \hat{S}^m)$
- 8:    $\tilde{P}_m \leftarrow \tilde{S}_m \tilde{S}_m^T$
- 9:    $\tilde{P}_m \leftarrow \tilde{P}_m^{\circ s}$
- 10: **end for**
- 11: **for**  $\tilde{P}_\star \in \{\tilde{P}, \tilde{P}_{\text{txt}}, \tilde{P}_{\text{img}}\}$  **do**
- 12:    $\tilde{P}_\star^f \leftarrow \sum_{k=1}^K \frac{a_k}{(\lambda^\star)^{k-1}} (\tilde{P}_\star - \lambda_{\min}^\star I)^k$  where  $\lambda_{\min}^\star$  is minimum eigenvalue of  $\tilde{P}_\star$
- 13: **end for**
- 14:  $\tilde{P}_{\text{MM}} \leftarrow \tilde{P}^f + \beta \tilde{P}_{\text{txt}}^f + \gamma \tilde{P}_{\text{img}}^f$
- 15:  $s_u \leftarrow r_u \tilde{P}_{\text{MM}}$
- 16: **return**  $s_u$

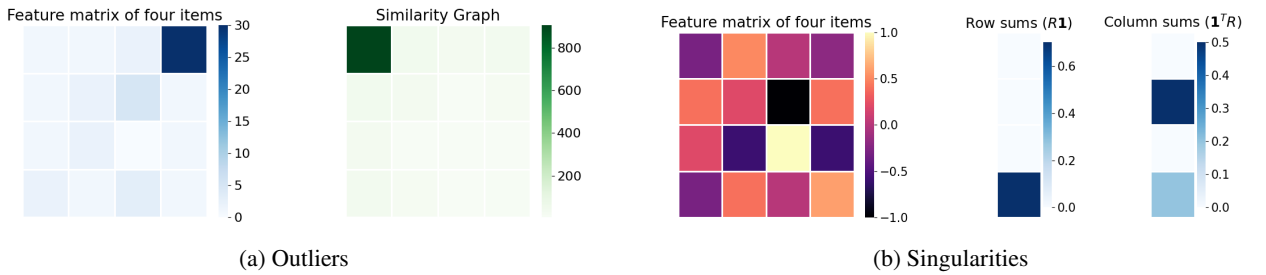


**Figure 4:** The impact of outliers and negative values (leading to singularities).

#### 4.2.1. Graph Construction for User–Item Interactions

Similarly as in existing GF-based recommendation methods (Kim et al., 2025; Park et al., 2024, 2025), the item–item similarity graph for user–item interactions is constructed as

$$\tilde{P} = \tilde{R}^T \tilde{R}; \quad \tilde{R} = D_r^{-\alpha} R D_c^{\alpha-1}, \quad (7)$$

where  $\alpha$  is a hyperparameter controlling the asymmetric normalization along users and items (Kim et al., 2025; Park et al., 2024, 2025). Additionally, we adjust  $\tilde{P}$  using the Hadamard power  $\tilde{P} = \tilde{P}^{\circ s}$  as properly adjusting the item–item similarity graph using the Hadamard power was shown to produce more accurate recommendations (Kim et al., 2025; Park et al., 2024, 2025), where  $\circ$  denotes the Hadamard (element-wise) power and  $s$  is a filter adjustment hyperparameter.

#### 4.2.2. Graph Construction for Textual and Visual Modalities

If we naïvely apply the same graph construction strategy used for user–item interactions to the textual and visual modalities, then we may fail due to the existence of *outliers* or *negative values* in feature vectors generated through sentence-transformers (Reimers and Gurevych, 2019) and pre-trained convolutional neural networks (CNNs) (He and McAuley, 2016a). As illustrated in Figure 4, constructing item–item similarity graphs for multimodal information using this strategy can lead to two critical issues. First, outliers in the feature vectors may cause certain elements of the graph to take excessively large values, thereby dominating the similarity graph and suppressing the contribution of other

similarities, which are then forced to remain close to zero (see Figure 4a). This distortion makes it difficult to accurately capture the true relationships between items. Second, when feature vectors include both positive and negative values, the row and column sums in the normalization process can approach zero (see Figure 4b). Dividing by such near-zero values results in singularities in the normalized graph, ultimately leading to instability and unreliable graph structures. Therefore, it is necessary to construct a graph structure in the form of similarity graphs tailored for multimodal information. While there exist a variety of similarity calculation strategies such as the Pearson correlation coefficient (Cohen et al., 2009) and the Gaussian kernel (Shuman et al., 2013), we empirically found that cosine similarity-based calculation guarantees superior performance on benchmark datasets in terms of recommendation accuracy consistently. In this context, we adopt cosine similarity to construct item–item similarity graphs unless otherwise stated.

To be specific, following (Yu et al., 2023; Zhang et al., 2021; Zhou and Shen, 2023), MM-GF constructs an item–item similarity graph by applying  $k$ NN sparsification on raw features corresponding to each modality  $m$ . Given  $N$  items, the similarity score  $S_{i,j}^m$  between item  $i$  and  $j$  is computed using cosine similarity based on their raw modality- $m$  feature vectors  $(x_i^m, x_j^m)$ , as follows:

$$S_{i,j}^m = \frac{x_i^m(x_j^m)^T}{\|x_i^m\| \|x_j^m\|}. \quad (8)$$

Here,  $S_{i,j}^m$  represents the element located at the  $i$ -th row and  $j$ -th column of the similarity matrix  $S^m \in \mathbb{R}^{N \times N}$ . To sparsify the graph, we apply  $k$ -nearest neighbor preservation in (Zhou and Shen, 2023) to convert the weighted matrix  $S^m$  into an unweighted version. For each item  $i$ , only its top- $k$  most similar neighbors are kept, resulting in the binary matrix  $\hat{S}^m$  defined by:

$$\hat{S}_{i,j}^m = \begin{cases} 1, & \text{if } S_{i,j}^m \in \text{top-}k(S_i^m), \\ 0, & \text{otherwise,} \end{cases} \quad (9)$$

where  $\hat{S}^m$  is the binarized matrix. Finally, the resulting feature matrix  $\hat{S}^m$  is then normalized to construct the item–item similarity graph  $\tilde{P}_m$  for modality  $m$ :

$$\tilde{P}_m = \tilde{S}_m \tilde{S}_m^T; \quad \tilde{S}_m = D_{m,r}^{-\alpha} \hat{S}^m D_{m,c}^{\alpha-1}, \quad (10)$$

where  $D_{m,r} = \text{diag}(\hat{S}^m \mathbf{1})$  and  $D_{m,c} = \text{diag}(\mathbf{1}^T \hat{S}^m)$  are the diagonal degree matrices for modality  $m$ . Likewise, we adjust  $\tilde{P}_m$  as  $\bar{P}_m = \tilde{P}_m^{\text{os}}$  in the graph construction process.<sup>1</sup>

#### 4.2.3. Filter Design with Multiple Modalities

Next, we are interested in how to precisely adjust the frequency bound of item–item similarity graphs. Specifically, when we adopt polynomial graph filters in (Kim et al., 2025; Park et al., 2024, 2025), it is necessary that all eigenvalues of the item–item similarity graph lie within  $[0, 1]$ . This approach defines a polynomial graph filter as  $\sum_{k=1}^K a_k \bar{P}_\star^k$ , which corresponds to the frequency response function  $h(\lambda) = \sum_{k=1}^K a_k (1 - \lambda)^k$ . However, as we observed in Figure 2 of Section 4.1, certain eigenvalues exceed the specified bounds.

To address the issue, we propose a more appropriate and technically valid polynomial graph filter by replacing  $\bar{P}_\star$  with  $\bar{P}_\star - \lambda_{\min}^* I$  and further normalizing each term by  $(\lambda^*)^{k-1}$  to control the spectral scaling, where  $\bar{P}_\star \in \{\bar{P}, \bar{P}_{\text{txt}}, \bar{P}_{\text{img}}\}$  and  $\lambda_{\min}^*$  is the minimum eigenvalue of  $\bar{P}_\star$ . This ensures that all eigenvalues of  $\bar{P}_\star - \lambda_{\min}^* I$  lie within the range  $[0, \lambda^*]$  where  $\lambda^* = \lambda_{\max}^* - \lambda_{\min}^*$  and  $\lambda_{\min}^*$  is the minimum eigenvalue of  $\bar{P}_\star$ .<sup>2</sup> To this end, we would like to establish the following theorem, which characterizes the frequency response function of a polynomial graph filter that accommodates the bounded range of eigenvalues.

**Theorem 4.1.** *For any admissible range of eigenvalues, the matrix polynomial can be expressed as:*

<sup>1</sup>While using different  $\alpha$ 's and  $s$ 's for each modality certainly increases recommendation accuracy, we use the same values of  $\alpha$  and  $s$  as those for user–item interactions across multiple modalities for simplicity.

<sup>2</sup> $\lambda_{\max}^*$  and  $\lambda_{\min}^*$  are obtained by solving the characteristic equation  $p(\lambda) = \det(\bar{P}_\star - \lambda I)$ .

$$\bar{P}_\star^f = \sum_{k=1}^K \frac{a_k}{(\lambda^\star)^{k-1}} (\bar{P}_\star - \lambda_{\min}^\star I)^k, \quad (11)$$

where  $\bar{P}_\star^f$  is the graph filter associated with the similarity graph  $\bar{P}_\star$ , having the frequency response function of  $h(\lambda) = \sum_{k=1}^K \frac{a_k}{(\lambda^\star)^{k-1}} (\lambda^\star - \lambda)^k$ , and  $\lambda^\star = \lambda_{\max}^\star - \lambda_{\min}^\star$ . Here,  $\lambda_{\min}^\star$  and  $\lambda_{\max}^\star$  are the minimum and maximum eigenvalues of  $\bar{P}_\star$ , respectively.

PROOF. First, we define the graph Laplacian  $L_\star$  for a specific modality  $\star$  as follows:

$$\bar{L}_\star = \lambda_{\max}^\star I - \bar{P}_\star = U \Lambda^\star U^T, \quad (12)$$

where  $\Lambda^\star$  is a set of eigenvalues of  $L_\star$ . Since the eigenvalues of  $\bar{P}_\star$  fall within  $[\lambda_{\min}^\star, \lambda_{\max}^\star]$ , those of  $L_\star$  lie within  $[0, \lambda^\star]$ . Based on the graph Laplacian  $L_\star$ , we have

$$\begin{aligned} \bar{P}_\star - \lambda_{\min}^\star I &= \lambda_{\max}^\star I - L_\star - \lambda_{\min}^\star I \\ &= U(\lambda_{\max}^\star I - \Lambda^\star - \lambda_{\min}^\star I)U^T \\ &= U(\lambda^\star I - \Lambda^\star)U^T, \end{aligned} \quad (13)$$

which implies that  $\bar{P}_\star - \lambda_{\min}^\star I$  is a graph filter having a frequency response function of  $h(\lambda) = \lambda^\star - \lambda$  for  $[0, \lambda^\star]$ . This corresponds to a linear LPF whose frequency response defined over the interval  $[0, \lambda^\star]$ . Now, we consider the  $k$ th-order polynomial filter. Then, we have

$$\begin{aligned} \frac{1}{(\lambda^\star)^{k-1}} (\bar{P}_\star - \lambda_{\min}^\star I)^k &= \frac{1}{(\lambda^\star)^{k-1}} \underbrace{U(\lambda^\star I - \Lambda^\star)U^T \dots U(\lambda^\star I - \Lambda^\star)U^T}_{k \text{ times}} \\ &= U \left( \frac{(\lambda^\star I - \Lambda^\star)^k}{(\lambda^\star)^{k-1}} \right) U^T, \end{aligned} \quad (14)$$

which indicates a graph filter with a frequency response function of  $h(\lambda) = \frac{(\lambda^\star - \lambda)^k}{(\lambda^\star)^{k-1}}$  for  $\lambda \in [0, \lambda^\star]$ . Since  $h(0) = \lambda^\star$ ,  $h(\lambda^\star) = 0$ , and  $h(\lambda)$  is a monotonically decreasing function in the interval  $[0, \lambda^\star]$ , the filtered value is still bounded in  $[0, \lambda^\star]$ . Therefore, the proposed filter design guarantees spectral boundedness of  $\bar{P}_\star^f$  within  $[0, \lambda^\star]$ , even when eigenvalues of  $\bar{P}_\star$  exceed the standard unit interval. This completes the proof of this theorem.  $\square$

While directly computing the coefficients  $a_k$  in Eq. (11) provides precise control over the frequency response, it also restricts flexibility because the coefficients are fixed in advance. To enhance flexibility, we treat  $a_k$  as tunable hyperparameters, allowing data-driven selection through validation rather than adhering to a fixed analytic form.

Finally, MM-GF optimally fuses multimodal information as a weighted sum of the graph filters across different modalities:

$$\bar{P}_{\text{MM}} = \bar{P}^f + \beta \bar{P}_{\text{txt}}^f + \gamma \bar{P}_{\text{img}}^f, \quad (15)$$

where  $\beta$  and  $\gamma$  are hyperparameters balancing among the three similarity graphs. The filtered signal for user  $u$  (i.e., the predicted preference scores of user  $u$ ) is finally given by

$$s_u = r_u \bar{P}_{\text{MM}}, \quad (16)$$

where  $r_u$  denotes the  $u$ -th row of  $R$  and is utilized as the graph signal for user  $u$ .

**Table 2**

The statistics of three benchmark datasets.

Dataset	# of users	# of items	# of interactions	Sparsity
Baby	19,445	7,050	160,792	99.88%
Sports	35,598	18,357	296,337	99.95%
Clothing	39,387	23,033	278,677	99.97%

**Table 3**

Performance comparison among MM-GF and competitors. The best and second-best performers are highlighted in bold and underline, respectively.

Method	Baby				Sports				Clothing			
	Recall@10	NDCG@10	Recall@20	NDCG@20	Recall@10	NDCG@10	Recall@20	NDCG@20	Recall@10	NDCG@10	Recall@20	NDCG@20
LightGCN	0.0479	0.0257	0.0754	0.0328	0.0569	0.0311	0.0864	0.0387	0.0340	0.0188	0.0526	0.0236
VBPR	0.0423	0.0223	0.0663	0.0284	0.0558	0.0307	0.0856	0.0384	0.0280	0.0159	0.0414	0.0193
GRCN	0.0539	0.0288	0.0833	0.0363	0.0598	0.0332	0.0915	0.0414	0.0424	0.0225	0.0650	0.0283
LATTICE	0.0547	0.0292	0.0850	0.0370	0.0620	0.0335	0.0953	0.0421	0.0492	0.0268	0.0733	0.0330
BM3	0.0564	0.0301	0.0883	0.0383	0.0656	0.0355	0.0980	0.0438	0.0421	0.0228	0.0625	0.0280
FREEDOM	<u>0.0627</u>	0.0330	<u>0.0992</u>	0.0424	0.0717	0.0385	0.1089	0.0481	0.0629	0.0341	0.0941	0.0420
MGCN	0.0620	<u>0.0339</u>	0.0964	<u>0.0427</u>	<u>0.0729</u>	<u>0.0397</u>	<u>0.1106</u>	<u>0.0496</u>	<u>0.0641</u>	<u>0.0347</u>	<u>0.0945</u>	<u>0.0428</u>
<b>MM-GF</b>	<b>0.0757</b>	<b>0.0432</b>	<b>0.1109</b>	<b>0.0522</b>	<b>0.0849</b>	<b>0.0495</b>	<b>0.1226</b>	<b>0.0593</b>	<b>0.0761</b>	<b>0.0424</b>	<b>0.1108</b>	<b>0.0513</b>

## 5. Experimental Results and Analyses

In this section, we systematically conduct extensive experiments to answer the following key five research questions (RQs).

- **RQ1:** How does MM-GF perform compared with the state-of-the-art multimodal recommendation methods?
- **RQ2:** How efficient is MM-GF in terms of runtime and scalability for multimodal recommendations?
- **RQ3:** How does each component of MM-GF affect its recommendation accuracy?
- **RQ4:** How does MM-GF perform in cold-start settings?
- **RQ5:** How sensitive is MM-GF under noisy multimodal data settings?
- **RQ6:** How sensitive is MM-GF to variations in its hyperparameters?

### 5.1. Experimental Settings

**Datasets.** We use three widely used benchmark datasets in recent MRSs (Yu et al., 2023; Zhang et al., 2021; Zhou et al., 2023a; Zhou and Shen, 2023), which were collected from Amazon (McAuley et al., 2015): (a) Baby, (b) Sports and Outdoors, and (c) Clothing, Shoes, and Jewelry, which we refer to as Baby, Sports, and Clothing, respectively, in brief.<sup>3</sup> The above three datasets contain textual and visual features as well as user–item interactions. For the textual modality, we use 384-dimensional textual embeddings by combining the title, descriptions, categories, and brand of each item and adopt sentence-transformers (Reimers and Gurevych, 2019). For the visual modality, we use 4,096-dimensional visual embeddings obtained by applying pre-trained CNNs (He and McAuley, 2016a). Table 1 provides a summary of the statistics for each dataset.

**Competitors.** To validate the effectiveness of MM-GF, we conduct a comparative analysis with seven state-of-the-art recommendation methods, especially those built upon neural network models including GCNs. The benchmark methods include not only a single-modal recommendation method (LightGCN (He et al., 2020)) but also multimodal recommendation methods (VBPR (He and McAuley, 2016b), GRCN (Wei et al., 2020), LATTICE (Zhang et al., 2021), BM3 (Zhou et al., 2023b), FREEDOM (Zhou and Shen, 2023), and MGCN (Yu et al., 2023)).

**Evaluation protocols.** We use the same dataset split for training, test, and validation sets, as well as the textual and visual data processing for feature extraction, as those in previous studies (Yu et al., 2023; Zhang et al., 2021; Zhou

<sup>3</sup>Datasets are officially available at <https://jmcauley.ucsd.edu/data/amazon/links.html>.

**Table 4**

Runtime comparison among MM-GF and representative GCN-based competitors. The best performer is highlighted in bold. NDCG refers to NDCG@20.

Method	Baby		Sports		Clothing	
	NDCG	Time	NDCG	Time	NDCG	Time
GRCN	0.0363	3h8m	0.0414	5h34m	0.0283	6h14m
LATTICE	0.0370	2h19m	0.0421	17h44m	0.0330	8h56m
BM3	0.0383	1h27m	0.0438	2h55m	0.0280	2h39m
MGCN	0.0427	13m33s	0.0496	58m4s	0.0428	53m11s
MM-GF	<b>0.0522</b>	<b>8.1s</b>	<b>0.0593</b>	<b>1m16s</b>	<b>0.0513</b>	<b>2m14s</b>

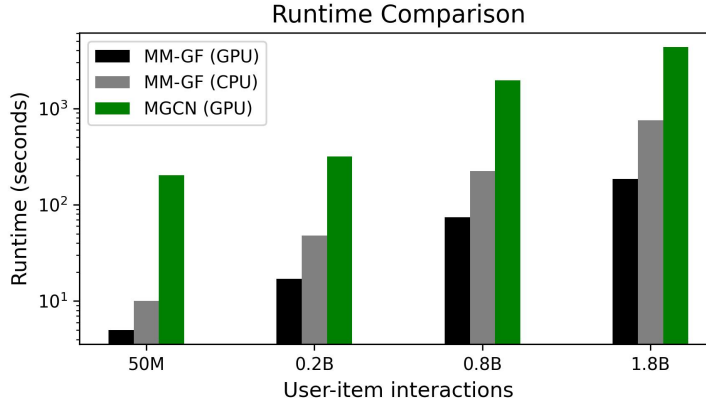


**Figure 5:** Log-scaled runtime comparison of MM-GF (with GPU and CPU) and MGCN (GPU) using various scaled synthetic datasets.

and Shen, 2023). To assess the top- $K$  recommendation performance, we adopt the widely used metrics from prior studies (He and McAuley, 2016b; He et al., 2020; Park et al., 2024; Shen et al., 2021; Wei et al., 2020; Yu et al., 2023; Zhang et al., 2021; Zhou and Shen, 2023; Zhou et al., 2023b), namely recall and normalized discounted cumulative gain (NDCG), where  $K \in \{10, 20\}$ . From RQ2 to RQ6 except RQ4, we report the results only for NDCG@20 as similar trends are observed for other metrics.

**Implementation details.** For a fair comparison, we implement the proposed MM-GF method and all benchmark methods using MMRec (Zhou, 2023), an open-sourced multimodal recommendation framework.<sup>4</sup> Unless otherwise stated, for MM-GF, the best-performing hyperparameters ( $a_1, a_2, a_3, \beta, \gamma$ ) in Eqs. (11) and (15) are set to  $(-0.7, 1.1, -0.1, 0.1, 0)$ ,  $(0.7, 1.8, 1.5, 1.9, 0.5)$ , and  $(1.9, 0.7, -0.1, 0.5, 0.2)$  for the Baby, Sports, and Clothing datasets, respectively, using the validation set. Additionally, we apply the proposed polynomial graph filter to the user-item interaction matrix, restricting the expansion to the third order (i.e.,  $K = 3$  in Eq. (11)). For the textual and visual modalities, we adopt a linear LPF, specified as  $\bar{P}_m^f = \bar{P}_m - \lambda_{min}^m I$ , for each modality  $m$ . These design choices are primarily guided by empirical evidence. The parameter  $k$  in Eq. (9) was empirically set to 20 in our experiments. All experiments are carried out on a machine with Intel (R) 12-Core (TM) i7-9700K CPUs @ 3.60 GHz and an NVIDIA GeForce RTX A6000 GPU.

## 5.2. Recommendation Accuracy (RQ1)

Table 3 summarizes the recommendation accuracy among MM-GF and seven recommendation competitors. Our observations are made as follows:

- (i) Compared to state-of-the-art recommendation methods, MM-GF consistently achieves superior performance across all datasets and metrics. Notably, on the Baby dataset, MM-GF achieves up to a gain of 13.35% in NDCG@20 over the second-best performer. This indicates that our nontrivial refinement for multimodal features and their effective fusion for GF enable us to achieve outstanding performance in MRSs.

<sup>4</sup>The toolbox is available at <https://github.com/enoch/MMRec>.

**Table 5**

Performance comparison among MM-GF and its four variants in terms of NDCG@20. The best performer is highlighted in bold.

Dataset	MM-GF	MM-GF-t	MM-GF-tv	MM-GF-pf	MM-GF-f
Baby	<b>0.0522</b>	0.0448	0.0448	0.0484	0.0420
Sports	<b>0.0593</b>	0.0493	0.0485	0.0562	0.0486
Clothing	<b>0.0513</b>	0.0377	0.0348	0.0445	0.0308

- (ii) The GCN-based methods (LightGCN, GRCN, LATTICE, BM3, FREEDOM, and MGCN) generally outperform the non-GCN method (VBPR), highlighting the effectiveness of explicitly capturing high-order relations through the message passing mechanism in MRSs.
- (iii) Among the GCN-based methods, those utilizing multimodal information (GRCN, LATTICE, BM3, FREEDOM, and MGCN) exhibit better performance than their counterpart, i.e., the single-modal recommendation method (LightGCN). This underscores the importance of incorporating multimodal information for enhanced recommendation accuracy.

### 5.3. Runtime and Scalability (RQ2)

Table 4 summarizes the runtime of MM-GF and GCN-based competitors that perform well (GRCN, LATTICE, BM3, and MGCN) on the three datasets. For the GCN-based methods, runtime refers to the training time, whereas, for the GF-based method (MM-GF), it indicates the processing time, as in (Park et al., 2024; Shen et al., 2021). We observe that, on the Baby dataset, MM-GF performs approximately  $\times 100.4$  faster than MGCN, which is the best GCN-based multimodal recommendation method, while exhibiting even higher recommendation accuracy. This is because MM-GF operates solely on straightforward matrix calculations without a costly training process. A similar tendency is observed on other two datasets. In consequence, the proposed MM-GF method is advantageous in terms of runtime as well as recommendation accuracy.

Furthermore, we compare the scalability of MM-GF and MGCN, which is the fastest and best-performing one out of GCN-based methods. We present a runtime comparison on different devices (i.e., CPU and GPU), using various scaled datasets. To this end, we generate four synthetic datasets whose sparsity is identically set to 99.99%, similarly as in three real-world benchmark datasets, i.e., Baby, Sports, and Clothing. More specifically, the numbers of (users, items, interactions) are set to  $\{(10k, 5k, 5k), (20k, 10k, 20k), (40k, 20k, 80k), (60k, 30k, 180k)\}$ . Additionally, to match the dimensionality of the feature embeddings, we set the dimensionality of textual and visual features to 384 and 4,096, respectively. As shown in Fig. 5, MM-GF has significantly shorter runtime than that of MGCN for all datasets and device configurations. Interestingly, running MM-GF with CPU is even faster than the case of MGCN with GPU. We also observe that MM-GF with GPU takes at most few minutes, while MGCN takes a minimum of several minutes and a maximum of several hours.

### 5.4. Ablation Study (RQ3)

We perform an ablation study to assess the contribution of each component in MM-GF. The performance comparison among MM-GF and its four variants is summarized in Table 5.

- MM-GF : preserves all components with no removal;
- MM-GF-t : excludes the textual feature (i.e.,  $\beta = 0$ );
- MM-GF-tv : excludes the textual and visual features (i.e.,  $\beta = \gamma = 0$ );
- MM-GF-pf : excludes the polynomial filter for user–item interaction data (i.e., adopts a linear LPF);
- MM-GF-f : setting of tunable hyperparameter  $a_k$  in Eq. (11) and rather uses the fixed coefficients as in (Kim et al., 2025; Park et al., 2024, 2025).

Our observations are made as follows:

- (i) The presence of multimodal information significantly contributes to performance improvement for all cases. In particular, the textual modality has a substantial impact on recommendation accuracy.

**Table 6**

Performance comparison among MM-GF and competitors in cold-start setting. The best and second-best performers are highlighted in bold and underline, respectively.

Method	Baby				Sports				Clothing			
	Recall@10	NDCG@10	Recall@20	NDCG@20	Recall@10	NDCG@10	Recall@20	NDCG@20	Recall@10	NDCG@10	Recall@20	NDCG@20
LightGCN	0.0400	0.0216	0.0646	0.0278	0.0434	0.0236	0.0642	0.0288	0.0256	0.0143	0.0380	0.0174
VBPR	0.0199	0.0111	0.0320	0.0138	0.0205	0.0113	0.0302	0.0138	0.0196	0.0102	0.0308	0.0130
GRCN	0.0301	0.0158	0.0480	0.0203	0.0342	0.0180	0.0543	0.0230	0.0306	0.0161	0.0474	0.0203
LATTICE	0.0424	0.0234	0.0656	0.0292	0.0525	0.0285	0.0771	0.0347	0.0481	0.0267	0.0679	0.0317
BM3	0.0323	0.0165	0.0468	0.0202	0.0425	0.0237	0.0603	0.0281	0.0261	0.0146	0.0363	0.0172
FREEDOM	0.0463	0.0258	<u>0.0711</u>	<u>0.0321</u>	0.0604	0.0328	0.0909	0.0404	0.0591	0.0323	<u>0.0883</u>	<u>0.0396</u>
MGCN	<u>0.0482</u>	<u>0.0259</u>	0.0700	0.0313	<u>0.0619</u>	<u>0.0351</u>	0.0900	<u>0.0422</u>	0.0540	0.0302	0.0771	0.0361
<b>MM-GF</b>	<b>0.0629</b>	<b>0.0349</b>	<b>0.0928</b>	<b>0.0424</b>	<b>0.0757</b>	<b>0.0433</b>	<b>0.1056</b>	<b>0.0509</b>	<b>0.0673</b>	<b>0.0362</b>	<b>0.0975</b>	<b>0.0439</b>

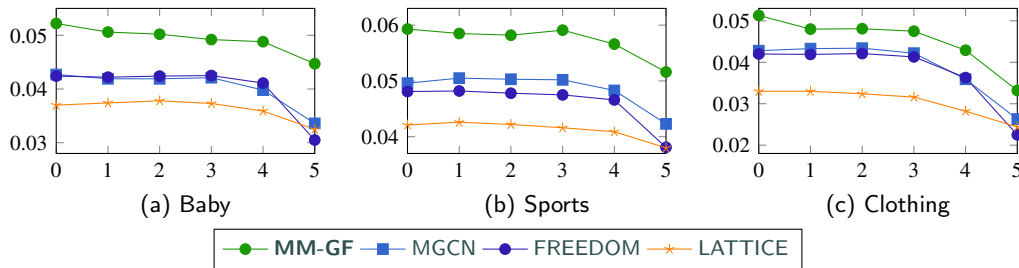


**Figure 6:** Performance comparison according to different degrees of noise. Here, the horizontal axis indicates the noise level  $x \in \{0, 1, 2, \dots, 5\}$ , which is specified in Section 5.6. The vertical axis means NDCG@20.

- (ii) As evidenced by the results of both MM-GF-t and MM-GF-tv, the gain of further leveraging the visual modality over MM-GF-t is indeed marginal; such a pattern was also comprehensively discussed in the earlier study in (Zhou et al., 2023a).
- (iii) The performance degradation in MM-GF-pf demonstrates that our modality-specific polynomial filter design contributes to the improvement of performance. Moreover, handling the bound of frequencies is essential for accurate predictions, as MM-GF-f leads to a considerable drop in performance.

### 5.5. Analysis in Cold-Start Settings (RQ4)

While high sparsity in graphs leads to technical challenges for model training, leveraging additional features in MRSs can enhance the recommendation accuracy in sparse conditions, as demonstrated by cold-start experiments (Zhou et al., 2023a). In this study, we regard the cold-start users as those who have rated equal to or fewer than 5 items. Hence, we only use such cold-start users on three benchmark datasets for model inference. The performance comparison among MM-GF and seven state-of-art multimodal recommendation competitors in cold-start settings is summarized in Table 6.<sup>5</sup> Our observations are made as follows:

- (i) Compared to the GCN-based methods (LightGCN, GRCN, LATTICE, BM3, FREEDOM, and MGCN), MM-GF still consistently achieves superior performance across all datasets and metrics (except for the Recall@20 on Clothing). Notably, on the Baby dataset, MM-GF achieves up to a gain of 35.46% in NDCG@20 over the best competitor.
- (ii) In comparison with Table 3, the previous multimodal recommendation methods such as VBPR, GRCN, and BM3 have a large performance decrease, showing vulnerability to cold-start settings. On the other hand, our MM-GF method has a marginal performance decrease in cold-start experiments. This finding demonstrates the robustness of our MM-GF method to cold-start settings.

<sup>5</sup>Since the datasets in cold-start settings differ from the original ones, we determine the optimal hyperparameters for each dataset under these settings.

## Graph Filtering for Multimodal Recommendation

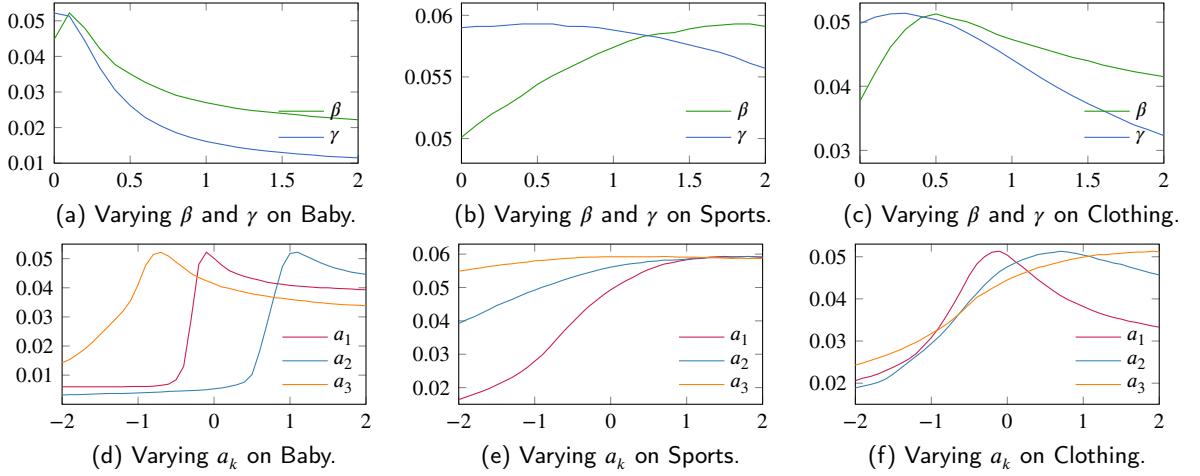


**Figure 7:** The effect of various hyperparameters for three benchmark datasets, where the horizontal and vertical axes indicate the value of each hyperparameter and the performance in NDCG@20, respectively. Each plot varies a single hyperparameter while keeping the others fixed.

### 5.6. Robustness to Noisy Multimodal Features (RQ5)

We analyze the sensitivity of noise that often occurs in real-world scenarios (Zhou et al., 2023a). In MRSs, multimodal features are vulnerable to noise due to various factors such as embedding inaccuracies or inconsistencies in data collection processes. To validate the robustness of MM-GF to such noisy multimodal features, we characterize the noise  $n$  as  $\tilde{X}_m^n = \tilde{X}_m + n$ , where  $n$  follows  $\mathcal{N}(0, \sigma_m^2)$  for the standard deviation  $\sigma_m$ . We define six different levels of noise according to different levels of the standard deviation: level 0 corresponds to the case where there is no noise, which represents the original datasets; level 1 corresponds to the noise equivalent to 10% of the standard deviation of each feature embedding; and as noise gets gradually added, level 5 corresponds to the noise that is twice the standard deviation of each feature embedding.

Figure 5.6 clearly shows that as the multimodal information incorporates more noise, all the competitors exhibit a decreasing trend in NDCG@20. In particular, MGCN (Yu et al., 2023) purifies the modality features to prevent noise contamination, which is a method directly designed for noise removal. In contrast, MM-GF consistently reveals the best performance in MRSs through only matrix computations without any noise-purification design. In other words, MM-GF exhibits robustness to noise with a simple yet effective multimodal feature process.

### 5.7. Hyperparameter Sensitivity

We analyze the sensitivity of MM-GF on the performance in NDCG@20 to variations in the key hyperparameters  $\beta, \gamma$ , and  $a_k$  in Figure 7.<sup>6</sup> Our observations are made as follows:

- (i) Setting  $\beta$  and  $\gamma$  to positive values generally leads to higher accuracies than the case of  $\beta = 0$  and  $\gamma = 0$ , thus validating the effectiveness of leveraging both textual and visual features for GF.
- (ii) As shown in Figure 7a, there is a monotonically decreasing pattern with increasing  $\gamma$ . That is, using visual features in MM-GF is rather harmful for multimodal recommendations, which is consistent with the earlier work in (Zhou et al., 2023a) that confirmed that not all multimodal information contributes to performance improvement.
- (iii) While the optimal values of hyperparameters differ across datasets and necessitate a broad search range, MM-GF is inherently less sensitive to hyperparameter choices and allows for rapid tuning. This is in contrast to training-based methods (Wei et al., 2020; Yu et al., 2023; Zhang et al., 2021; Zhou and Shen, 2023), which often demand costly and time-consuming optimization procedures. Our model’s simplicity enables efficient deployment even with minimal tuning effort.

<sup>6</sup>We note that the differing scales of  $\beta$  and  $\gamma$  in the optimization process stem from the heterogeneous nature of multimodal features, while the variations in  $a_k$  arise from the flexibility of the polynomial filter design.

## 6. Conclusions and Outlook

In this paper, we proposed MM-GF, the first training-free multimodal recommendation method grounded in the concept of GF, aiming for both efficiency and accuracy. MM-GF effectively adjusted the spectral bounds of frequencies, alongside a flexible and spectrally-aware graph filtering strategy. By integrating modality-specific similarity graphs with a tunable polynomial graph filter, our MM-GF method was shown to enable precise frequency control and robust fusion of heterogeneous information. Extensive experimental evaluations demonstrated not only the remarkably fast runtime of MM-GF but also the superior recommendation accuracy of MM-GF in diverse challenging scenarios, including cold-start conditions and resilience to noisy features. Avenues of future research include the design of scalable GF methods that accommodate large-scale multi-modal feature data.

## Acknowledgments

This work was supported in part by the National Research Foundation of Korea (NRF) grant funded by Korea government (MSIT) under Grants RS-2021-NR059723 and RS-2023-00220762.

## References

- Cohen, I., Huang, Y., Chen, J., Benesty, J., Benesty, J., Chen, J., Huang, Y., Cohen, I., 2009. Pearson correlation coefficient, in: Noise Reduction Speech Processing, Springer. pp. 1–4.
- Defferrard, M., Bresson, X., Vandergheynst, P., 2016. Convolutional neural networks on graphs with fast localized spectral filtering, in: Proc. Int. Conf. Neural Inf. Process. Syst., Barcelona, Spain. pp. 3837–3845.
- Grone, R., Merris, R., 1994. The Laplacian spectrum of a graph II. SIAM J. Discret. Math. 7, 221–229. doi:10.1137/S0895480191222653.
- Guo, Z., Li, J., Li, G., Wang, C., Shi, S., Ruan, B., 2024. Lgmrec: Local and global graph learning for multimodal recommendation, in: Proc. 38th AAAI Conf. Artif. Intell. (AAAI'24), Vancouver, Canada, pp. 8454–8462. doi:10.1609/AAAI.V38I8.28688.
- He, R., McAuley, J.J., 2016a. Ups and downs: Modeling the visual evolution of fashion trends with one-class collaborative filtering, in: Proc. The Web Conf. (WWW'16), Montreal, Canada. pp. 507–517. doi:10.1145/2872427.2883037.
- He, R., McAuley, J.J., 2016b. VBPR: Visual Bayesian personalized ranking from implicit feedback, in: Proc. 30th AAAI Conf. Artif. Intell. (AAAI'16), Phoenix, AZ. pp. 144–150. doi:10.1609/AAAI.V30I1.9973.
- He, X., Deng, K., Wang, X., Li, Y., Zhang, Y., Wang, M., 2020. LightGCN: Simplifying and powering graph convolution network for recommendation, in: Proc. 43rd Int. ACM Conf. Res. Develop. Inf. Retrieval (SIGIR'20), Virtual Event. pp. 639–648. doi:10.1145/3397271.3401063.
- Isufi, E., Gama, F., Shuman, D.I., Segarra, S., 2024. Graph filters for signal processing and machine learning on graphs. IEEE Trans. Signal Process. 72, 4745–4781. doi:10.1109/TSP.2024.3349788.
- Ju, B., Qian, Y., Ye, M., Ni, R., Zhu, C., 2015. Using dynamic multi-task non-negative matrix factorization to detect the evolution of user preferences in collaborative filtering. PLoS one 10, e0135090.
- Kim, C., Choi, Y., Park, J., Shin, W., 2025. Leveraging member-group relations via multi-view graph filtering for effective group recommendation, in: Proc. The Web Conf. (WWW'25), ACM. pp. 1077–1081. doi:10.1145/3701716.3715482.
- Kim, Y., Kim, T., Shin, W., Kim, S., 2024. MONET: modality-embracing graph convolutional network and target-aware attention for multimedia recommendation, in: Proc. of 17th ACM Int. Conf. Web Search and Data Mining (WSDM'24), ACM. pp. 332–340. doi:10.1145/3616855.3635817.
- Kipf, T.N., Welling, M., 2017. Semi-supervised classification with graph convolutional networks, in: Proc. 5th Int. Conf. Learn. Representations (ICLR'17), Toulon, France.
- Liu, J., Li, D., Gu, H., Lu, T., Zhang, P., Shang, L., Gu, N., 2023. Personalized graph signal processing for collaborative filtering, in: Proc. The Web Conf. (WWW'23), Austin, TX. pp. 1264–1272. doi:10.1145/3543507.3583466.
- McAuley, J.J., Targett, C., Shi, Q., van den Hengel, A., 2015. Image-based recommendations on styles and substitutes, in: Proc. 38th Int. ACM Conf. Res. Develop. Inf. Retrieval (SIGIR'15), Santiago, Chile. pp. 43–52. doi:10.1145/2766462.2767755.
- Ortega, A., Frossard, P., Kovacevic, J., Moura, J.M.F., Vandergheynst, P., 2018. Graph signal processing: Overview, challenges, and applications. Proc. IEEE 106, 808–828. doi:10.1109/JPROC.2018.2820126.
- Park, J., Shin, Y., Shin, W., 2024. Turbo-CF: Matrix decomposition-free graph filtering for fast recommendation, in: Proc. 47th Int. ACM Conf. Res. Develop. Inf. Retrieval (SIGIR'24), Washington D.C., USA. pp. 2672–2676. doi:10.1145/3626772.3657916.
- Park, J., Yoo, J., Shin, W., 2025. Criteria-aware graph filtering: Extremely fast yet accurate multi-criteria recommendation, in: Proc. The Web Conf. (WWW'25), ACM. pp. 4482–4493. doi:10.1145/3696410.3714799.
- Pereira, F.S.F., Gama, J., de Amo, S., Oliveira, G.M.B., 2018. On analyzing user preference dynamics with temporal social networks. Mach. Learn. 107, 1745–1773. doi:10.1007/S10994-018-5740-2.
- Ranjbar, M., Moradi, P., Azami, M., Jalili, M., 2015. An imputation-based matrix factorization method for improving accuracy of collaborative filtering systems. Eng. Appl. Artif. Intell. 46, 58–66. doi:10.1016/J.ENGAPPAI.2015.08.010.
- Reimers, N., Gurevych, I., 2019. Sentence-BERT: Sentence embeddings using siamese BERT-networks, in: Proc. Conf. on Empirical Methods Natural Lang. Process., 9th Int. Joint Conf. Natural Lang. Process. (EMNLP-IJCNLP'19), Hong Kong, China. pp. 3980–3990. doi:10.18653/V1/D19-1410.

- Rendle, S., Freudenthaler, C., Gantner, Z., Schmidt-Thieme, L., 2012. BPR: Bayesian personalized ranking from implicit feedback. CoRR abs/1205.2618. URL: <http://arxiv.org/abs/1205.2618>, arXiv:1205.2618.
- Shen, Y., Wu, Y., Zhang, Y., Shan, C., Zhang, J., Letaief, K.B., Li, D., 2021. How powerful is graph convolution for recommendation?, in: Proc. 30th Int. Conf. Inf. Knowl. Manage. (CIKM'21), Virtual Event. pp. 1619–1629. doi:10.1145/3459637.3482264.
- Shuman, D.I., Narang, S.K., Frossard, P., Ortega, A., Vandergheynst, P., 2013. The emerging field of signal processing on graphs: Extending high-dimensional data analysis to networks and other irregular domains. IEEE Signal Process. Mag. 30, 83–98. doi:10.1109/MSP.2012.2235192.
- Valcarce, D., Landin, A., Parapar, J., Barreiro, Á., 2019. Collaborative filtering embeddings for memory-based recommender systems. Eng. Appl. Artif. Intell. 85, 347–356. doi:10.1016/J.ENGAPPAI.2019.06.020.
- Wang, X., He, X., Wang, M., Feng, F., Chua, T., 2019. Neural graph collaborative filtering, in: Proc. 42nd Int. ACM Conf. Res. Develop. Inf. Retrieval, (SIGIR'19), Paris, France. pp. 165–174. doi:10.1145/3331184.3331267.
- Wei, Y., Wang, X., Nie, L., He, X., Chua, T., 2020. Graph-refined convolutional network for multimedia recommendation with implicit feedback, in: Proc. 28th ACM Int. Conf. Multimedia (MM'20), Virtual Event. pp. 3541–3549. doi:10.1145/3394171.3413556.
- Xia, J., Li, D., Gu, H., Liu, J., Lu, T., Gu, N., 2022. FIRE: fast incremental recommendation with graph signal processing, in: Proc. The Web Conf. (WWW'22), ACM. pp. 2360–2369. doi:10.1145/3485447.3512108.
- Xu, K., Hu, W., Leskovec, J., Jegelka, S., 2019. How powerful are graph neural networks?, in: Proc. 7th Int. Conf. Learn. Representations (ICLR'19), New Orleans, LA.
- Yu, P., Tan, Z., Lu, G., Bao, B., 2023. Multi-view graph convolutional network for multimedia recommendation, in: Proc. 31st ACM Int. Conf. Multimedia (MM'23), Ottawa, ON, Canada. pp. 6576–6585. doi:10.1145/3581783.3613915.
- Yu, P., Tan, Z., Lu, G., Bao, B., 2025. Mind individual information! principal graph learning for multimedia recommendation, in: Proc. 39th AAAI Conf. Artif. Intell. (AAAI'25), Philadelphia, PA, pp. 13096–13105. doi:10.1609/AAAI.V39I12.33429.
- Zhang, J., Zhu, Y., Liu, Q., Wu, S., Wang, S., Wang, L., 2021. Mining latent structures for multimedia recommendation, in: Proc. 29th ACM Int. Conf. Multimedia (MM'21), Virtual Event. pp. 3872–3880. doi:10.1145/3474085.3475259.
- Zhou, H., Zhou, X., Zeng, Z., Zhang, L., Shen, Z., 2023a. A comprehensive survey on multimodal recommender systems: Taxonomy, evaluation, and future directions. arXiv preprint arXiv:2302.04473 doi:10.48550/ARXIV.2302.04473.
- Zhou, X., 2023. MMRec: Simplifying multimodal recommendation, in: Proc. 5th Multimedia Asia Workshops (MMAsia'23), Tainan, Taiwan. pp. 6:1–6:2. doi:10.1145/3611380.3628561.
- Zhou, X., Shen, Z., 2023. A tale of two graphs: Freezing and denoising graph structures for multimodal recommendation, in: Proc. 31st ACM Int. Conf. Multimedia (MM'23), Ottawa, ON, Canada. pp. 935–943. doi:10.1145/3581783.3611943.
- Zhou, X., Zhou, H., Liu, Y., Zeng, Z., Miao, C., Wang, P., You, Y., Jiang, F., 2023b. Bootstrap latent representations for multi-modal recommendation, in: Proc. The Web Conf. (WWW'23), Austin, TX. pp. 845–854. doi:10.1145/3543507.3583251.